COMPDYN 2021
8th ECCOMAS Thematic Conference on
Computational Methods in Structural Dynamics and Earthquake Engineering
M. Papadrakakis, M. Fragiadakis (eds.)
Streamed from Athens, Greece, 27–30 June 2021

ANALYTICAL AND NUMERICAL MODELLING OF THE IN-PLANE RESPONSE OF TIMBER DIAPHRAGMS RETROFITTED WITH PLYWOOD PANELS

Michele Mirra[1], **Marianthi Sousamli**[2], **Michele Longo**[2], **Geert Ravenshorst**[1]

[1] Faculty of Civil Engineering and Geosciences – Section of Bio-Based Structures and Materials
Delft University of Technology
Stevinweg 1, 2628 CN Delft, The Netherlands
e-mail: m.mirra@tudelft.nl, g.j.p.ravenshorst@tudelft.nl

[2] Faculty of Civil Engineering and Geosciences – Section of Applied Mechanics
Delft University of Technology
Stevinweg 1, 2628 CN Delft, The Netherlands
e-mail: m.sousamli@tudelft.nl, m.longo@tudelft.nl

Abstract

In the region of Groningen (NL), human-induced earthquakes initiated by gas extraction are causing structural damage. In that area, the building stock is mainly composed of unreinforced masonry (URM) buildings with light and flexible timber floors and roofs. Thus, an experimental campaign was arranged for assessing the in-plane response of these diaphragms, and a retrofitting method was developed, consisting of an overlay of plywood panels screwed to the existing sheathing around their perimeter. This light, reversible stiffening measure showed a great increase in the in-plane strength, stiffness, and energy dissipation of the floors. Subsequently, an analytical model was developed, showing very good agreement with experimental results, and enabling the design of retrofitting interventions with this technique. Starting from the formulated model, a user-supplied subroutine was implemented in the finite element software DIANA FEA, allowing to represent the in-plane response of the diaphragms, including their energy dissipation. Finally, the impact of this retrofitting intervention on a case study of an existing building was evaluated by means of nonlinear time-history analyses. The results of numerical analyses show that the user-supplied subroutine accurately describes the in-plane behaviour of the retrofitted timber floors. Besides, the proposed retrofitting technique greatly increases the global seismic performance of the building, compared with both its as-built configuration and to stiffer and less reversible strengthening measures.

Keywords: Timber floors, Seismic Rehabilitation, Retrofitting, Seismic capacity, Masonry.

1 INTRODUCTION

In-plane response of timber diaphragms greatly influences the seismic response of existing unreinforced masonry (URM) buildings. As-built floors are often too flexible to withstand in-plane loads without causing the out-of-plane collapse of the walls. Hence, a proper retrofitting of the diaphragms, as well as an improvement of their connections to the walls, have to be performed. In this framework, several strengthening techniques have been investigated in the recent years [1]-[14], aiming at enhancing the seismic properties of the existing diaphragms. Among these techniques, reversible ones are usually preferred when they are applied to monumental structures, because of their lower impact [15].

Retrofitting interventions on timber diaphragms appear to be urgent and delicate in the region of Groningen, in the northern part of the Netherlands, where earthquakes induced by gas extraction are causing structural damage. The seismic events up to now have been light and have not caused collapses, but according to probabilistic studies, more intense events might occur. In that area, the building stock is mainly composed of URM low-rise buildings with light and flexible timber floors and roofs. This construction typology is widely present and very vulnerable to horizontal loads, because the buildings were not designed to withstand earthquakes, since seismic events were absent until recently. Thus, in 2018-19 a full-scale test campaign, recalled in Section 2, was arranged at Delft University of Technology for assessing the in-plane response of as-built and strengthened timber diaphragms typical of the Groningen area. The retrofitting measure consisted of an overlay of plywood panels screwed to the existing sheathing around their perimeter. This light, reversible strengthening measure showed a great increase in the in-plane strength, stiffness, and energy dissipation of the floors [14].

In this work, the analytical and numerical modelling of the refurbished floors is presented. An analytical model was firstly developed to enable a detailed design of the retrofitting intervention with the proposed strengthening technique. The formulated model, presented in detail in [16] and recalled in Section 3, estimates well the floors' strength, stiffness and energy dissipation, including pinching behaviour.

After these first steps, the impact of this retrofitting intervention in a case study of an existing building was evaluated by means of nonlinear time-history analyses. Three configurations were studied: an as-built one with flexible floors; one where a stiff and not reversible retrofitting intervention was applied, such as the cast of a concrete slab on the existing diaphragms; one where the proposed strengthening method was applied. For the latter case, given the high amount of energy dissipation of floors already at limited in-plane deflection, and their characteristic pinching behaviour, it was important to model in detail their seismic response for fully evaluating the impact of this retrofitting method. For this purpose, starting from the developed analytical model, a user-supplied subroutine was implemented in the finite element software DIANA FEA [17], allowing to represent the global in-plane response of the diaphragms. In this way, it was possible to simulate the nonlinear behaviour of both masonry (already featured by the software) and timber floors. The subroutine implementation is presented in Section 4, while results from the analyses on the case-study building are discussed in Section 5.

2 IN-PLANE EXPERIMENTAL TESTS ON TIMBER DIAPHRAGMS

To gain more insight into the in-plane behaviour of timber diaphragms with Dutch features, an experimental campaign was arranged at Delft University of Technology [14]. The floors were initially tested in their as-built configuration, and then retested after being strengthened with an overlay of plywood panels screwed along their perimeter to the existing sheathing. Prior to testing, portions of diaphragms were extracted from existing buildings in the Groningen area, so that the material properties of the tested samples could be accurately replicat-

ed and representative for the actual floors. Five full-scale samples representing half of a floor were tested in a vertical configuration (Fig. 1): two specimens were tested parallel to the joists (*DFpar-1*, *DFpar-2*) and two perpendicular to them (*DFper-3*, *DFper-4*), the last represented a roof pitch (*DRpar-5*). For the strengthened samples, the same nomenclature was adopted, adding the letter *s* at the end of each specimen name. As can be noticed from Fig. 1, the retrofitted floors exhibited a great improvement in strength, stiffness, and energy dissipation. To facilitate a detailed design of retrofitting interventions by adopting the proposed strengthening technique, an analytical model was formulated, which is presented in the next section. For further details on this experimental campaign, the reader can refer to [14].

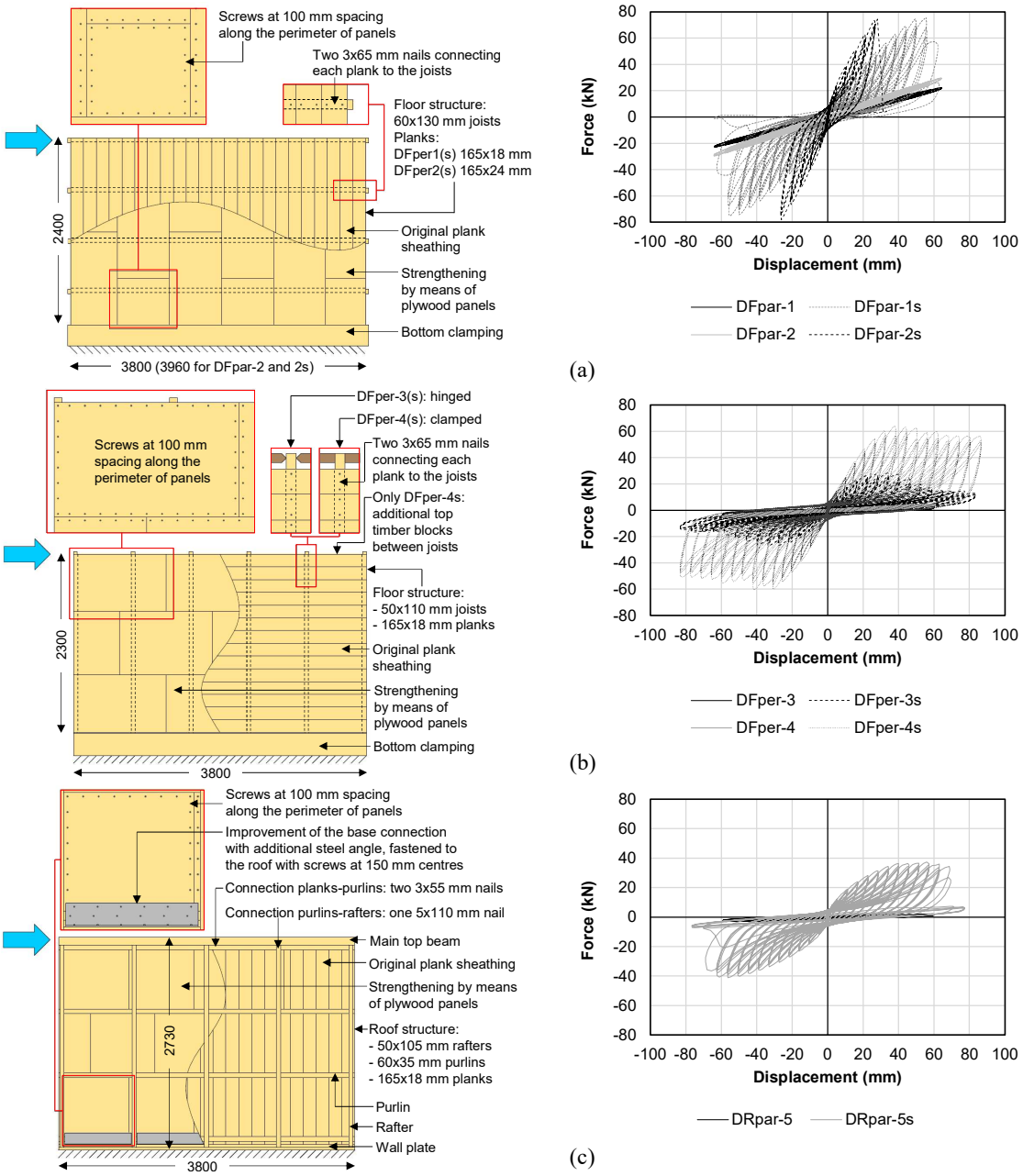

Figure 1: Main characteristics and cyclic in-plane response of the timber diaphragms; floors tested parallel (a) and perpendicular to the joists (b), roof pitch (c) [14].

3 ANALYTICAL MODELLING OF THE STRENGTHENED DIAPHRAGMS

3.1 General

The starting point for the formulation of the model was the evaluation of the load-slip behaviour of the screws fastening planks and plywood panels (Section 3.2). Based on their response, the global in-plane response of the diaphragm was then derived analytically (Section 3.3). The developed calculation model enables a good prediction of the diaphragms' in-plane behaviour [16], as shown in Section 3.4.

3.2 Evaluation of the load-slip behaviour of the fasteners

Besides the experimental campaign on full-scale floors, tests were also performed on fourteen small-size replicates for evaluating the response of the screws connecting plywood panels and planks. These specimens were composed of a plank and a plywood panel portion fastened together by means of two screws (Fig. 2). The samples were tested in shear, under the quasi-static reversed-cyclic loading protocol of ISO 16670 [18]: seven replicates were tested parallel to the main direction of the plank, and the other seven orthogonal to it (Fig. 2a). Similar load-slip curves were obtained between the two loading directions (Fig. 3).

Based on the obtained results, the load-slip response was modelled by means of a combination of a linear and a parabolic branch, representing the initial stiffness and the global behaviour, respectively [16]. A continuous curve was created with an extension of Foschi's load-slip model for nails [19]. With the proposed model, both post-yielding and softening behaviour of the fasteners can be described. The equation of the curve was defined as follows:

$$F_s = (F_0 + a\, d_s + b\, d_s^2)[1 - \exp(-K_0\, d_s/F_0)] \geq 0; \text{ with } a > 0,\ b < 0 \qquad (1)$$

In Eq. 1, F_s and d_s are the force and displacement of the screw, respectively; F_0, a and b are the coefficients of the parabola representing the global behaviour, while K_0 is the slope of the line representing the initial stiffness. This curve fits the experimental points with $R^2 = 0.83$ when the panel is loaded parallel to the plank, and with $R^2 = 0.95$ if the force is applied perpendicular to it (Fig. 3). As a failure criterion, the ultimate displacement was considered as the one for which the transferred load drops below 80% of the peak strength during the softening phase, in agreement with the provisions of ISO 16670 [18] and EN 12512 [20]. As a last consideration, a scatter is present in the data points and the backbones, as it is usually observed when analysing tests on timber joints. Yet, since a large number of screws is used in the whole floor, the global behaviour will approach the average trend.

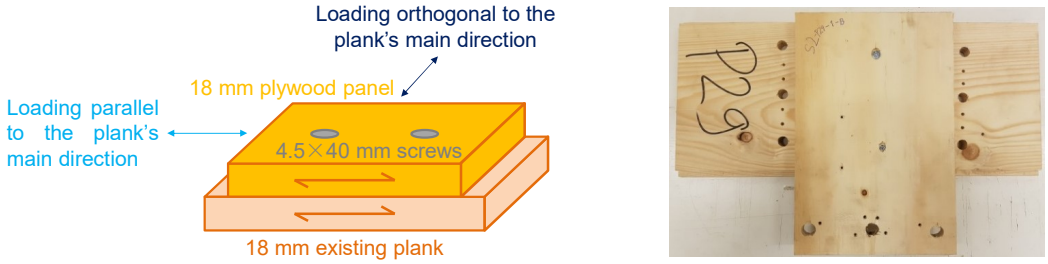

Figure 2: Samples prepared for testing the screws fastening the plywood panels to the existing sheathing: schematic description (a) and example of specimen (b) [16].

With the aforementioned procedure, it is possible to construct the load-slip curve starting from experimental tests, but in order to further generalize the proposed model, a fully analytical estimation of the curve was proposed as well [16]. This generalization was also necessary because some of the full-scale strengthened floors had different characteristics from the small-size replicates: sample *DFpar-2s* featured 24 mm planks, and in specimens *DFpar-2s*, *DFper-3s*, *DFper-4s* screws with a 5 mm diameter were used [14]. Therefore, the parameters K_0, F_0, a and b were also estimated according to formulations from standards or literature.

The initial stiffness K_0 was found to be well predicted with the expression provided in [21] for non-predrilled nails, thus $K_0 = 50\ d^{1.7}$, with d nominal diameter of the screw.

F_0 can be predicted starting from the knowledge of the maximum force F_{max} determined according to EN 1995 [22] and Johansen's theory [23] for timber-to-timber joints, and with a screw sufficiently slender to develop two plastic hinges. Then, F_0 can be estimated as $F_{max}/8$ (Fig. 4).

To determine the parameters a and b, three points crossed by the parabola have to be identified. The last quantity to be estimated is thus the slip d_{max} of the screw at F_{max}. To this end, firstly the expression of EN 409 [24] can be used for determining the angle α at which the screws' bending moment is evaluated, and adopting for its calculation the shank or inner diameter d_1 of the screw. Secondly, the distance $(b_1 + b_2)$ between the two plastic hinges according to Johansen's theory [23] is determined. By combining these two quantities, the slip at F_{max} can be estimated as $d_{max} = (b_1 + b_2)\tan(\alpha)$ (Fig. 4). The parabola is thus now identified by the three points $(0, F_0)$, (d_{max}, F_{max}), and $(2d_{max}, F_0)$. Further details on the analytical derivation of the proposed load-slip curve can be found in [16].

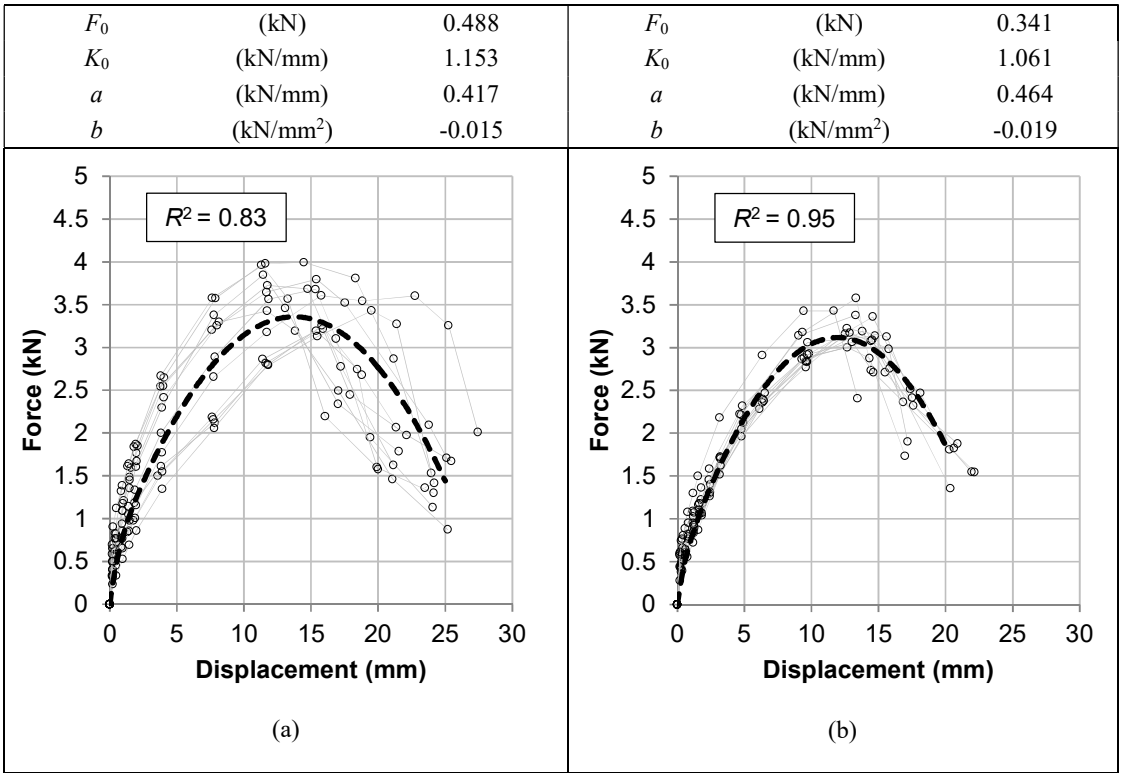

Figure 3: Proposed load-slip curve (dashed) in comparison to experimental data points and backbones for the direction parallel (a) and perpendicular to planks (b). The main parameters of the equation are also reported [16].

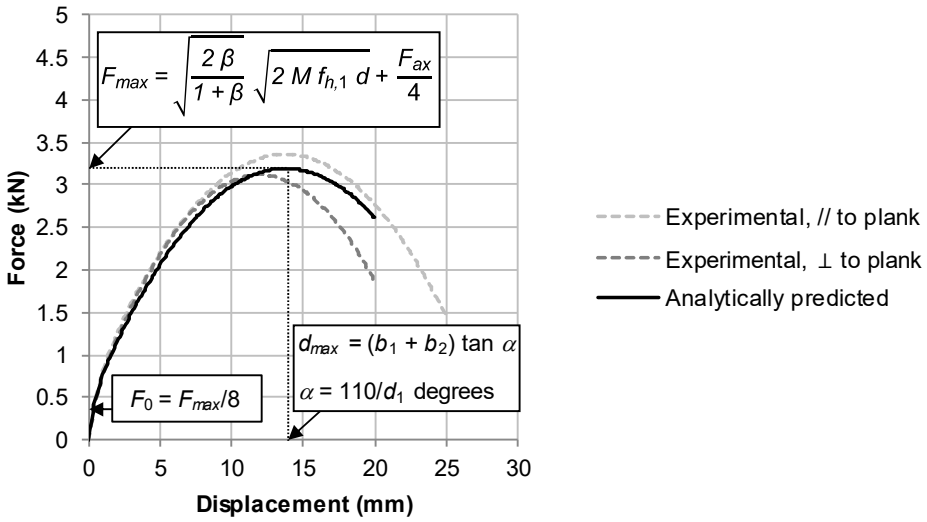

Figure 4: Comparison between the analytically derived curve and the ones obtained from the experimental data [16]. In the reported equations, the same notation as in EN 1995 [22] and EN 409 [24] is used.

3.3 Prediction of the global response of the retrofitted diaphragms

The floors were retrofitted by screwing plywood panels along their perimeter to the existing sheathing. This type of refurbishment is particularly advantageous, because the screws are placed in such a way that it is possible to identify their specific contribution to the overall resisting mechanism. With reference to Fig. 5, when the strengthened floor is subjected to a horizontal load and the panels are vertically arranged, the force is subdivided among the columns of panels, and the screws are opposing to it with their stiffness. Each column of panels is subjected to rotation and sliding: the rocking behaviour is taken into account by considering the vertical screws, while the (very limited) slip is evaluated through the horizontal screws (Fig. 5). In general, the diaphragms retrofitted with this method can be regarded as very similar to timber shear walls. Therefore, once the load-slip response of the single screw is known, the global behaviour can be predicted by considering equilibrium relations [16].

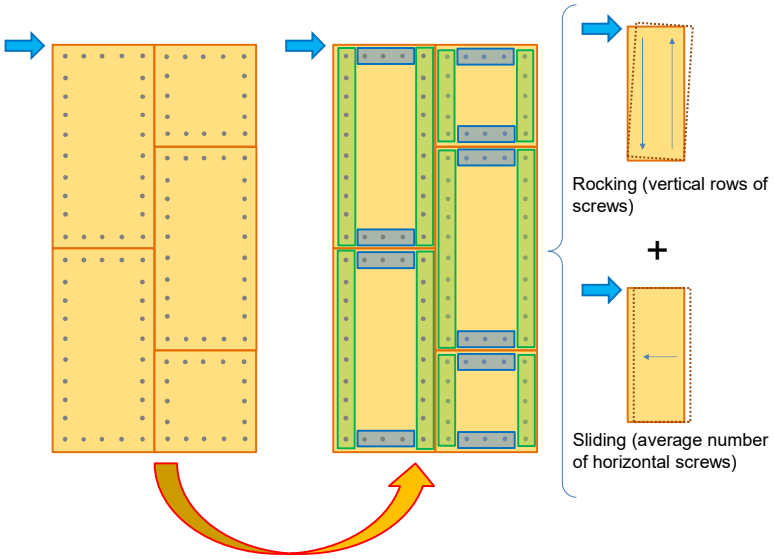

Figure 5: Determination of the global floors' response from single screws through equilibrium relations [16].

Additionally, the evaluation of energy dissipation was essential, because the strengthened diaphragms proved to provide significant values of equivalent hysteretic damping, of approximately 14-15% [25]. In order to consider this potentially beneficial effect in numerical modelling, an analytical formulation for determining the evolution of pinching cycles was proposed [16].

The pinching behaviour implies the presence of a residual force at zero displacement: this load approximately corresponds to the force causing the very first yielding of the tested sample. In the analytical curve equation, F_0 is the intercept on the y-axis (force) of the parabola representing the global response of the specimens. To capture the very first yielding on the analytical curve, the intercept on the y-axis assumed for the pinching cycle was $2/3F_0$, a value around which the initial slope of the curve starts to change.

Starting from this first intercept, the pinching cycle can be estimated for a certain amplitude identified by a point (δ_c, $F_c(\delta_c)$) on the curve. As a first step, two lines are determined: one joining the points (0, $2/3F_0$) and (δ_c, $F_c(\delta_c)$), and one crossing the point (δ_c, $F_c(\delta_c)$) with slope K_0 (Fig. 6, step 1). Then, the bisector of these two lines is found (step 2). In step 3, the remaining part of the cycle is defined: firstly, the line joining (0, $2/3F_0$) and the point on the bisector having x-coordinate equal to $\delta_c/2$ is determined; secondly, a line parallel to the former one intersects the branch having slope K_0, starting from the point (0, $-2/3F_0$).

In step 4, the whole multilinear cycle is determined, and could already be used for software implementation, as it was exemplified in [16]. The negative part of the pinching cycle (points B', C', D' of Fig. 6) is antisymmetric to the positive one, as is assumed for the backbone curve equation. For a more refined evaluation of both pinching and damping properties of the diaphragms, this multilinear cycle is used in step 5 to construct four exponential branches, smoothening the straight lines, again similarly to Foschi's formulation. The equations of these branches are reported in Section 4.3, in which the implementation of the user-supplied subroutine is presented. A graphical representation of them is given in step 6 of Fig. 6, showing the pinching cycles evolution.

3.4 Comparison between analytical and experimental results

By combining the derived analytical curve and the pinching cycles estimation, the cyclic response of the tested diaphragms was predicted: the reliability of the developed model can now be evaluated by comparing the analytical results with experimental ones. Therefore, this section presents a comparison of the analytical backbone (always depicted in red) and an estimated representative pinching cycle (always shown in dark blue), with the experimental hysteretic cycles (light blue). The results are shown in Figs. 7-9 for a diaphragm tested parallel to the joists (sample *DFpar-1s*, Fig. 7), a floor tested perpendicular to the joists (sample *DFper-4s*, Fig. 8), and the roof pitch (Sample *DFper-5s*, Fig. 9); both the global behaviour and the initial response (up to 20 mm displacement) are displayed. For a more detailed comparison and overview, the reader is referred to [16]. As can be noticed, the analytical model proves to well predict the in-plane behaviour of all diaphragms, also when variations are present with respect to the reference tests on plank-plywood panel joints. In general, the initial stiffness and pinching response are accurately captured by the model, along with strength and displacement at failure of the specimens.

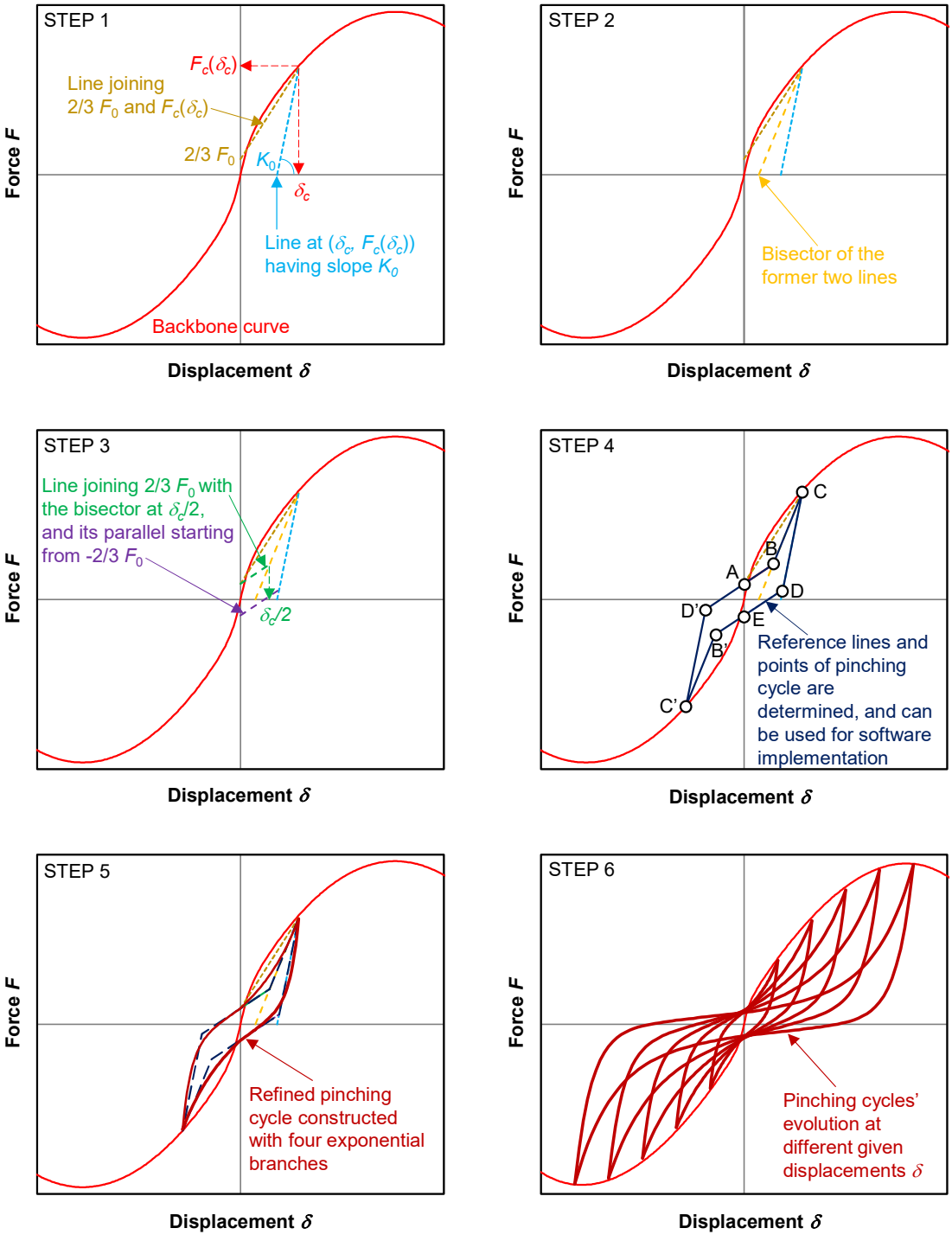

Figure 6: Procedure for the determination of the pinching cycles from the analytical backbone curve [16].

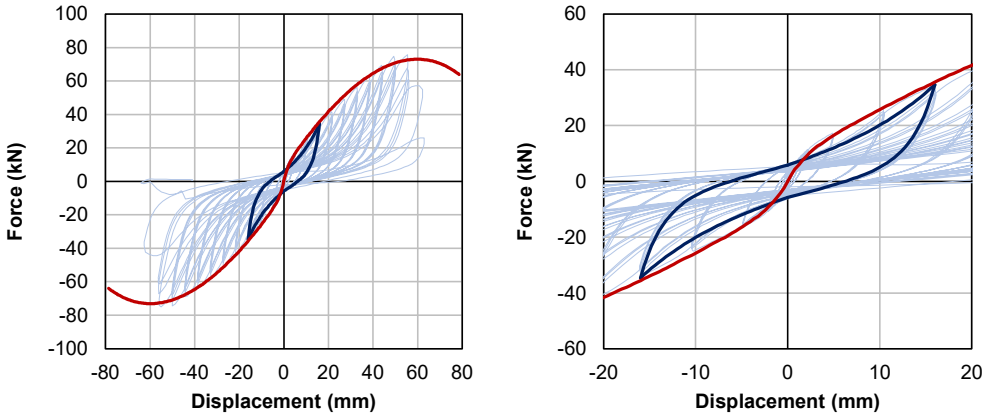

Figure 7: Comparison between analytical backbone (red) and a representative pinching cycle (dark blue) with the experimental hysteretic response (light blue) for sample *DFpar-1s*: global (left) and initial (right) response [16].

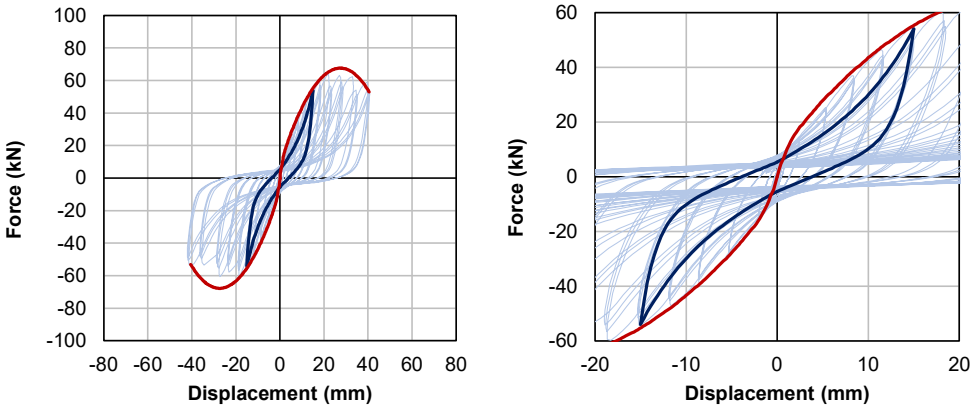

Figure 8: Comparison between analytical backbone (red) and a representative pinching cycle (dark blue) with the experimental hysteretic response (light blue) for sample *DFper-4s*: global (left) and initial (right) response [16].

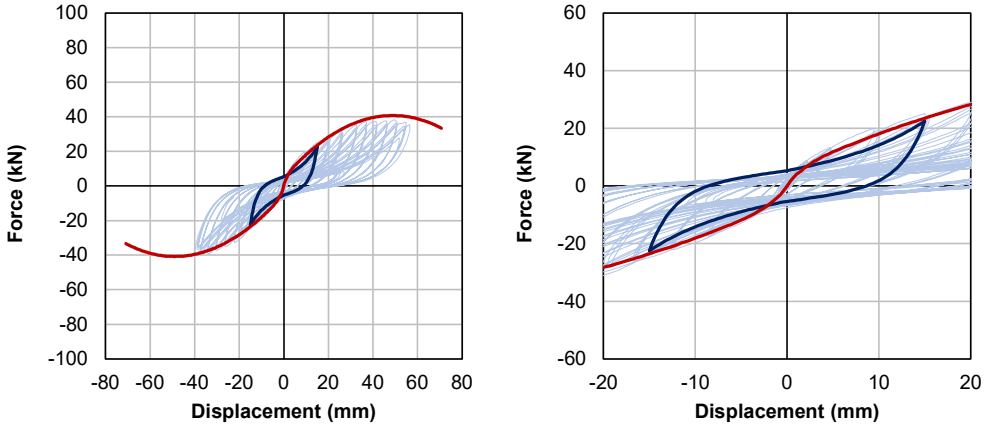

Figure 9: Comparison between analytical backbone (red) and a representative pinching cycle (dark blue) with the experimental hysteretic response (light blue) for sample *DFpar-5s*: global (left) and initial (right) response [16].

4 NUMERICAL MODELLING OF THE STRENGTHENED DIAPHRAGMS

4.1 General

Given the great improvement in relevant seismic properties of the retrofitted timber diaphragms, it was important to properly model their in-plane response. In this way, the potentially beneficial effect of their energy dissipation, provided at an already limited deflection, could be described. Yet, when considering existing URM buildings with timber floors, the behaviour of the diaphragms is usually simplified in numerical models. Existing or not stiff diaphragms are often modelled as (very flexible) linear elastic orthotropic slabs [26], while after retrofitting them the hypothesis of infinitely stiff diaphragms is frequently assumed, given its compliance with the pushover method [27].

Therefore, the potential energy dissipation of the floors is neglected, and their global in-plane response is not fully considered. However, if it is possible to properly account for both, then an optimized design of the retrofitted diaphragms could be achieved, so that the floors can become an additional source of energy dissipation for the buildings in which they are present. In order to further investigate these aspects, the aforementioned analytical model was implemented in a user-supplied subroutine to be imported in the software DIANA FEA, version 10.4 [17]. This software already featured an advanced nonlinear model for masonry, but lacked suitable materials and constitutive laws for modelling timber floors. In the following sections, the adopted modelling strategy, the subroutine implementation, and its validation are discussed.

4.2 Modelling strategy for timber floors

In order to properly capture the in-plane and out-of-plane behaviour of the diaphragms, while simultaneously implementing the analytical model, a macro-element strategy was adopted (Fig. 10). The floors were modelled by combining linear elastic shell elements, for representing the out-of-plane behaviour under static vertical loads, and nonlinear macro-elements overlapped to them for describing the in-plane behaviour.

These macro-elements consisted of six trusses: four rigid trusses connected to form a quadrilateral, and two nonlinear trusses placed diagonally (Fig. 10), in which the nonlinear in-plane behaviour of the floor was implemented adopting the proposed analytical model. This modelling strategy proved to be accurate and efficient, and was also adopted in past research studies [28], [29]. For the linear elastic orthotropic shells, the flexural characteristics were assigned considering an equivalence between the actual inertial properties of the joists, and those of the slab, so that the same vertical deflection could be achieved.

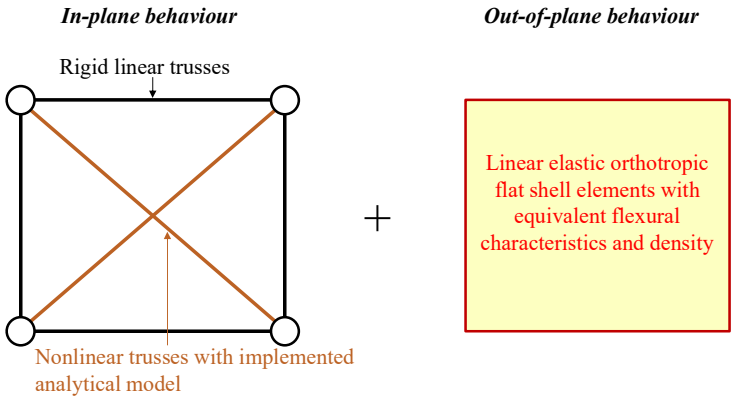

Figure 10: Adopted strategy for modelling in-plane and out-of-plane behaviour of timber diaphragms.

4.3 Implementation of the user-supplied subroutine

In order for the user-supplied subroutine to be compatible with the DIANA FEA environment, the constitutive laws for the diagonal trusses of the macro-elements were implemented adopting the FORTRAN 90 programming language. Two types of input variables are required by the software: user-specified initialization parameters (not changing within the subroutine calculations), and initial state variables (varying during subroutine calculations, e.g. for determining loading and unloading points). As output, DIANA FEA requires user-supplied subroutines to provide the stress-strain relation, to be adopted at every calculation step.

Three relevant parameters for initialization were chosen: the strain ε_{max} at peak stress σ_{max}, the peak stress σ_{max} itself, and the initial elastic modulus K_0 (Fig. 11). These parameters are known, once the retrofitting of the diaphragm is designed through the analytical model, according to the expected seismic loads. Besides, ten initial state variables were adopted, necessary for describing all loading and unloading branches, and their initial value was set to 0. With reference to Fig. 11, these variables are the maximum strains ever reached in tension and compression ($\varepsilon_{t,max}$ and $\varepsilon_{c,max}$, respectively), and the stress-strain coordinates identifying the end of the loading and unloading branches in tension (points $(\varepsilon_{t,l}, \sigma_{t,l})$ and $(\varepsilon_{t,ul}, \sigma_{t,ul})$, respectively) and compression (points $(\varepsilon_{c,l}, \sigma_{c,l})$ and $(\varepsilon_{c,ul}, \sigma_{c,ul})$, respectively). Through these variables, the pinching behaviour during unloading and reloading can be defined. The constitutive laws implemented through the user-supplied subroutine are now presented for the tensile branch only, since the compressive one follows antisymmetric relations.

The material follows the tensile loading branch as long as $\varepsilon > 0$ and $\varepsilon > \varepsilon_{t,max}$, with the constitutive law of Eq. 2 (Fig. 12, blue branch):

$$\sigma = (\sigma_y + a\,\varepsilon + b\,\varepsilon^2)[1 - \exp(-K_0\,\varepsilon/\sigma_y)] \tag{2}$$

In Eq. 2, $\sigma_y = \sigma_{max}/8$, following the analytical derivation presented in Section 3.2.

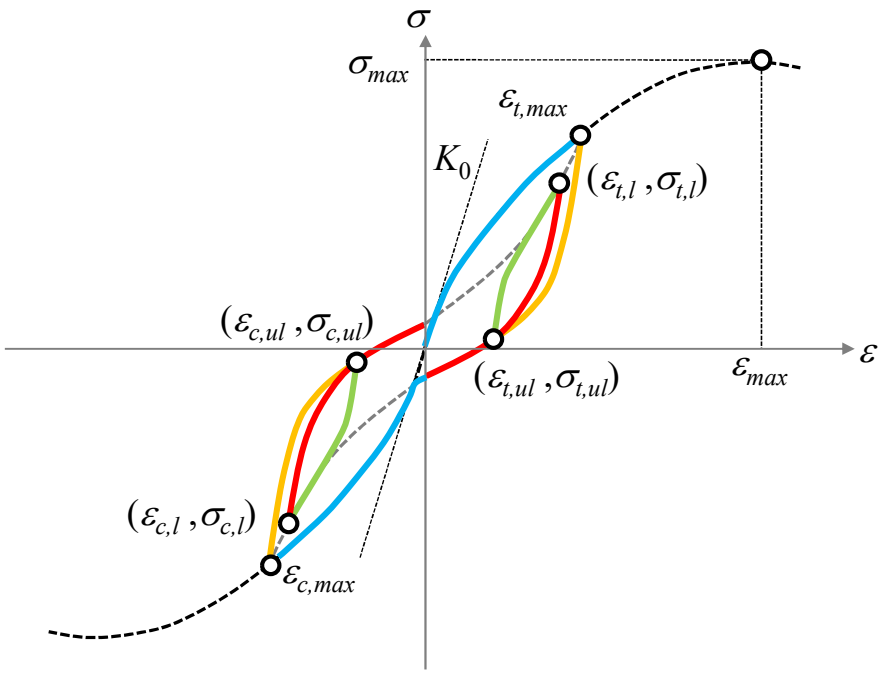

Figure 11: Representation of the input parameters for the user-supplied subroutine.

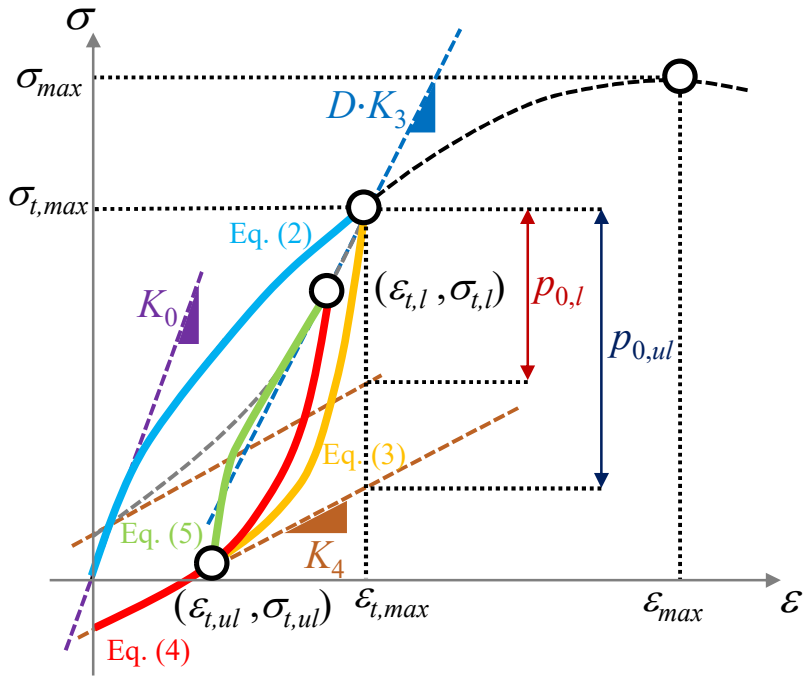

Figure 12: Loading, unloading and reloading branches implemented in the user-supplied subroutine.

After reaching $\varepsilon_{t,max}$, the tensile unloading phase is defined if $\varepsilon > 0$, $\varepsilon < \varepsilon_{t,max}$, and $\varepsilon < \varepsilon_0$, with ε_0 initial strain at the beginning of the current step. In this case, the response is distinguished between the case in which the unloading starts from the envelope curve (at $\varepsilon_{t,max}$, yellow branch of Fig. 12), and when the unloading occurs after a reloading phase (red branch of Fig. 12). In the first case, $\varepsilon_{t,l} \equiv \varepsilon_{t,max}$, and the constitutive law is formulated as (see Fig. 12 for the meaning of the various parameters):

$$\sigma = f_{t,ul} = \sigma_{t,max} - [\sigma_{t,max} - p_{0,ul} - K_4(\varepsilon - \varepsilon_{t,max})]\{1 - \exp[2K_0(\varepsilon - \varepsilon_{t,max})/(\sigma_{t,max} - p_{0,ul})]\} \quad (3)$$

In the second case, instead, the relation is ($\varepsilon_{t,l} \neq \varepsilon_{t,max}$):

$$\sigma = \sigma_{t,l} - (\sigma_{t,l} - f_{t,ul})\{1 - \exp[2K_0(\varepsilon - \varepsilon_{t,l})/(\sigma_{t,l} - f_{t,ul})]\} \quad (4)$$

Finally, the tensile reloading phase is defined if $\varepsilon > 0$, $\varepsilon < \varepsilon_{t,max}$, and $\varepsilon > \varepsilon_0$, according to the constitutive law of Eq. 5:

$$\sigma = \sigma_{t,ul} + (f_{t,l} - \sigma_{t,ul})\{1 - \exp[-2K_0(\varepsilon - \varepsilon_{t,ul})/(f_{t,l} - \sigma_{t,ul})]\} \quad (5)$$

with:

$$f_{t,l} = \sigma_{t,max} - [\sigma_{t,max} - p_{0,l} - K_4(\varepsilon - \varepsilon_{t,max})]\{1 - \exp[D \cdot K_3(\varepsilon - \varepsilon_{t,max})/(\sigma_{t,max} - p_{0,l})]\} \quad (6)$$

and:

$$D = 1 + (\varepsilon_{t,max}/\varepsilon_{max})^3 \quad (7)$$

With reference to Eq. 7, the parameter D is a factor accounting for the progressive degradation of the pinching cycles, becoming progressively less stiff when the floor drift increases (Fig. 6, step 6).

4.4 Validation of the user-supplied subroutine

As already presented in section 3.4, the analytical model proved to be accurate for predicting the global in-plane response of the retrofitted timber diaphragms. Since the model was implemented in the user-supplied subroutine, very close results were expected, useful to validate both the subroutine itself, and the adopted modelling strategy for timber diaphragms.

As validation example, a retrofitted timber diaphragm with similar characteristics to sample *DFpar-1s* was modelled. A 4×6 m floor was considered, supported on the long sides, having as in-plane properties an initial stiffness of 10 kN/mm, and a strength of 150 kN activated at 60 mm displacement. The floor featured 60×130 mm joists at a heart-to-heart distance of 500 mm, while the thickness of both plywood panels and planks was 18 mm. The elastic modulus of timber was assumed to be 10000 MPa. On the basis of these characteristics, equivalent input properties were determined for the elements in the numerical model.

The modelled diaphragm consisted of a mesh of 1×1 m macro-elements (capturing the in-plane response), overlapped to flat shell elements (accounting for the out-of-plane behaviour), as shown in Fig. 13. The three initial parameters, required by the user-supplied subroutine for determining the constitutive law of the nonlinear diagonal trusses, can be derived from geometrical considerations. Starting from the whole floor deflection u, the displacement δ of a truss is given by:

$$\delta = (u \cos \alpha)/m \tag{8}$$

where α is the angle between the truss and the loading direction (Fig. 13), and m the number of macro-elements rows parallel to the applied load in half of the floor (in this case, $m = 2$). The shear force $F/2$ is then subdivided among the s trusses in one macro-elements row, and transformed into an axial force N on a single one:

$$N = F/(2\, s \cos \alpha) \tag{9}$$

From the knowledge of the geometrical relations for N and δ, also the initial stiffness of the diagonal trusses can be calculated. For convenience, a unitary section was adopted for the truss elements, so that force and stress could be coincident in their values.

The properties of the shell elements were derived by considering an equivalence in flexural properties between the joists and the slab, defining an equivalent elastic modulus E_{eq}:

$$E_{eq} = E_{timber} I_{joists}/I_{slab} \tag{10}$$

where I_{joists} is the sum of the moments of inertia of the single joists, and I_{slab} is the moment of inertia of the slab, defined by attributing to the shell elements a thickness of 36 mm (planks and plywood panels). According to the reference system of Fig. 13, the elastic modulus E_{eq} was assigned to all directions, while the shear moduli were different: a value of 0.1 MPa was assigned to G_{xy}, because the in-plane behaviour was already described by the macro-elements, while $G_{xz} = G_{zy} = E_{eq}/16$ (similarly to an actual timber material). The main material properties assigned to the model are summarized in Table 1. Hinged supports were placed to the two lateral edges parallel to the application of the in-plane load (Fig. 13).

The floor was firstly subjected to a linear static analysis to verify the equivalence in flexural properties between the slab and the joists (Fig. 14a). Both the self-weight and a vertical load of 1.5 kN/m^2 were applied. Then, two in-plane cyclic analyses were performed, one to assess the global cyclic behaviour (Fig. 14b), and one in which local loops were imposed (Fig. 14c). These analyses were displacement-based, and the displacement was applied at the floor midspan (Fig. 13). Finally, a time-history analysis was conducted (Fig. 14d), subjecting the floor to a scaled seismic signal, representative for the Groningen area.

As can be noticed (Fig. 14), both out-of-plane and in-plane behaviour of the floor are properly captured by the adopted modelling strategy and the implemented subroutine. The deflection under vertical loads proved the correct application of the flexural properties to the shell elements: the obtained displacement was practically coincident with the one calculated analytically by considering the floor joists. With regard to the in-plane response, strength, stiffness, energy dissipation and pinching behaviour are well described in all in-plane analyses, with a response quite close to that of reference sample *DFpar-1s* (Fig. 7a).

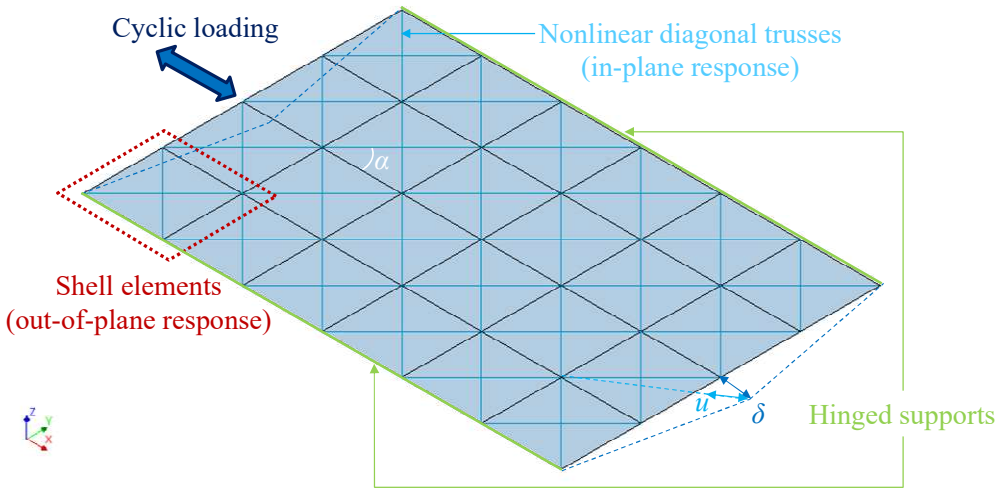

Figure 13: Model of the retrofitted diaphragm for the validation of the user-supplied subroutine.

Table 1: Properties adopted in the floor model.

Function	Element type	Property	Value
Macro-elements representing the in-plane behaviour of the floor	Rigid trusses	Elastic modulus E_t (MPa)	10^{10}
	Diagonal trusses	ε_{max}	0.01
		σ_{max} (MPa)	12000
		K_0 (MPa)	5520000
Shell elements describing the out-of-plane response of the floor	Shell elements	Elastic moduli E_x, E_y, E_z (MPa)	62000
		In-plane shear modulus G_{xy} (MPa)	0.1
		Shear moduli G_{xz}, G_{zy} (MPa)	3880

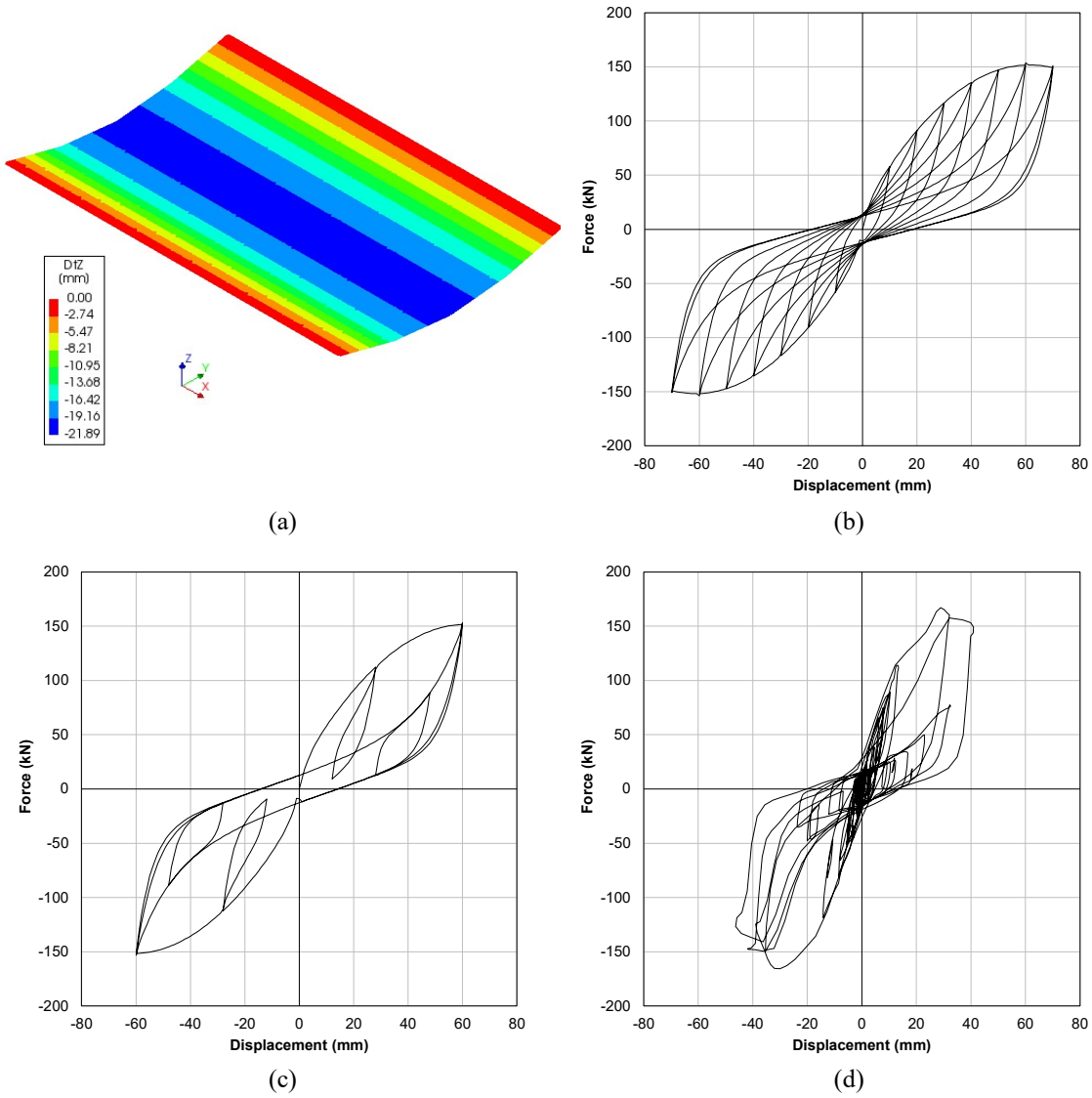

Figure 14: Results from the analyses conducted for the validation of the user-supplied subroutine and the overall modelling strategy for timber floors: out-of-plane static analysis under vertical loads (a); complete displacement-based in-plane cyclic analysis (b); displacement-based in-plane cyclic analysis with local loops (c); in-plane time-history analysis under an induced Groningen earthquake accelerogram (d).

5 CASE STUDY: A MASONRY DETACHED HOUSE WITH TIMBER FLOORS

5.1 Introduction

The implemented user-supplied subroutine opened up the opportunity to analyse the beneficial impact of a dissipative retrofitting of timber diaphragms in an existing URM building. The effect of floors strengthened with plywood panels, and thus with a light, reversible technique, was compared to that of the as-built configuration, and of another not reversible retrofitting measure, widely applied also in the past, and namely the cast of a reinforced concrete slab on the existing diaphragms. Several studies have already shown that the latter retrofitting measure could be detrimental for masonry buildings [28]-[30], and not advisable if the construction is protected or part of the architectural heritage of a certain context [15]. Yet, the

need of stiffening in their plane the existing, inadequate floors, combined with design rules based on the hypothesis of infinitely stiff diaphragms [27], could often result in realizing a concrete slab. This intervention undoubtedly increases the overall seismic masses, but contemporarily improves the static out-of-plane behaviour of the floor, and also the in-plane capacity of walls. After applying these retrofitting measures, or similar ones making the floors almost infinitely stiff, the contribution that is missing is the potential energy dissipation that the floors could provide. If, instead, the diaphragms are strengthened with a dissipative technique, allowing efficient shear transfer and horizontal loads redistribution, and at the same time a controlled deflection, then their role can be quite beneficial. With the adopted retrofitting solution, this advantageous effect can be obtained, and through the user-supplied subroutine it can be evaluated through numerical analyses, fully accounting for the nonlinear in-plane response of the floors.

5.2 Characteristics of the analysed building

A detached house typical of the Groningen area was selected as the case-study building (Fig. 15). This URM low-rise house has a relatively simple structure, but some irregularities are present, such as the position and shape of wall openings, and the thickness of the walls, not constant along the height, with gables featuring a single-leaf wall (100 mm thick) instead of the ground floor double-wythe walls (210 mm thick). Besides, one more single-leaf wall was present, supporting one of the floors approximately at midspan, in correspondence to the staircase (Fig. 15). Three configurations were studied: one represented the as-built house with flexible diaphragms; in the other two, the floors were retrofitted with plywood panels or with a concrete slab. The properties of masonry, reported in Table 2, were assumed to be the same for the three configurations. The adopted values are in line with the characteristics of medium-low quality masonry: these material properties fall on the conservative side with respect to experimental tests performed on both existing and replicated Dutch masonry [31], [32], and were also defined according to calibration studies [33]. Shell elements with the implemented DIANA FEA Engineering Masonry Model [34] were used for modelling the masonry.

For all configurations, nonlinear incremental dynamic analyses were performed, by subjecting the house to seven accelerograms of induced earthquakes retrieved from the seismic database of the Nederlands Normalisatie-instituut (NEN) [35]. The main loading directions x and y were studied separately, therefore a total of 42 analyses were performed. The signals were referred to an average peak ground acceleration (PGA) of 0.17g, and are shown in Fig. 16; a Rayleigh damping of 2% was considered in the analyses. While for walls a density of 2000 kg/m^3 was assumed, for the diaphragms the density values included the self-weight of structural elements, a dead load of 1.00 kN/m^2 (accounting for further elements such as non-structural walls, finishes, plants, pipes), and 30% of the live load, equal to 1.75 kN/m^2 for Dutch residential buildings [36].

The as-built configuration featured flexible diaphragms: the 4.0×4.6 m floor presented 75×180 mm joists at a heart-to-heart distance of 800 mm; the 4.6×6.8 m floor had 60×160 mm joists arranged at 750 mm heart-to-heart distance; the roof presented 50×105 mm rafters at 900 mm heart-to-heart distance; all diaphragms had 18 mm thick planks. These structural properties were translated in the numerical model by following the modelling strategy for shell elements described in Section 4.2. In this case, because of the very small energy dissipation observed from tests on replicated as-built floors [14], the diaphragms were modelled with linear elastic orthotropic shell elements (thus without overlapping the nonlinear macro-elements), whose properties are reported in Table 3. The in-plane shear moduli of the diaphragms were derived by considering the flexural properties of the planks or the joists [14]. These values would correspond to equivalent shear stiffnesses of 108 to 216 kN/m, and are

thus in line with other similar stiffness estimations for existing floors from literature [3], [4], [7], [8], [11]-[14]. From an in-situ inspection, it was noticed that a timber wall plate surrounded the whole roof, and the floor joists were also connected to this structure. Therefore, a continuous hinged connection was assumed between diaphragms and walls at the floors supports. A continuous connection among masonry walls was assumed as well. In general, the main elements of vulnerability due to the diaphragms flexibility, are related to the lack of seismic load redistribution among the walls in the *x* direction, and to the very low stiffness of the roof structure in the *y* direction, with possible local collapses of the north and south wall gables. These issues were confirmed by the observed failures, as discussed in the next section.

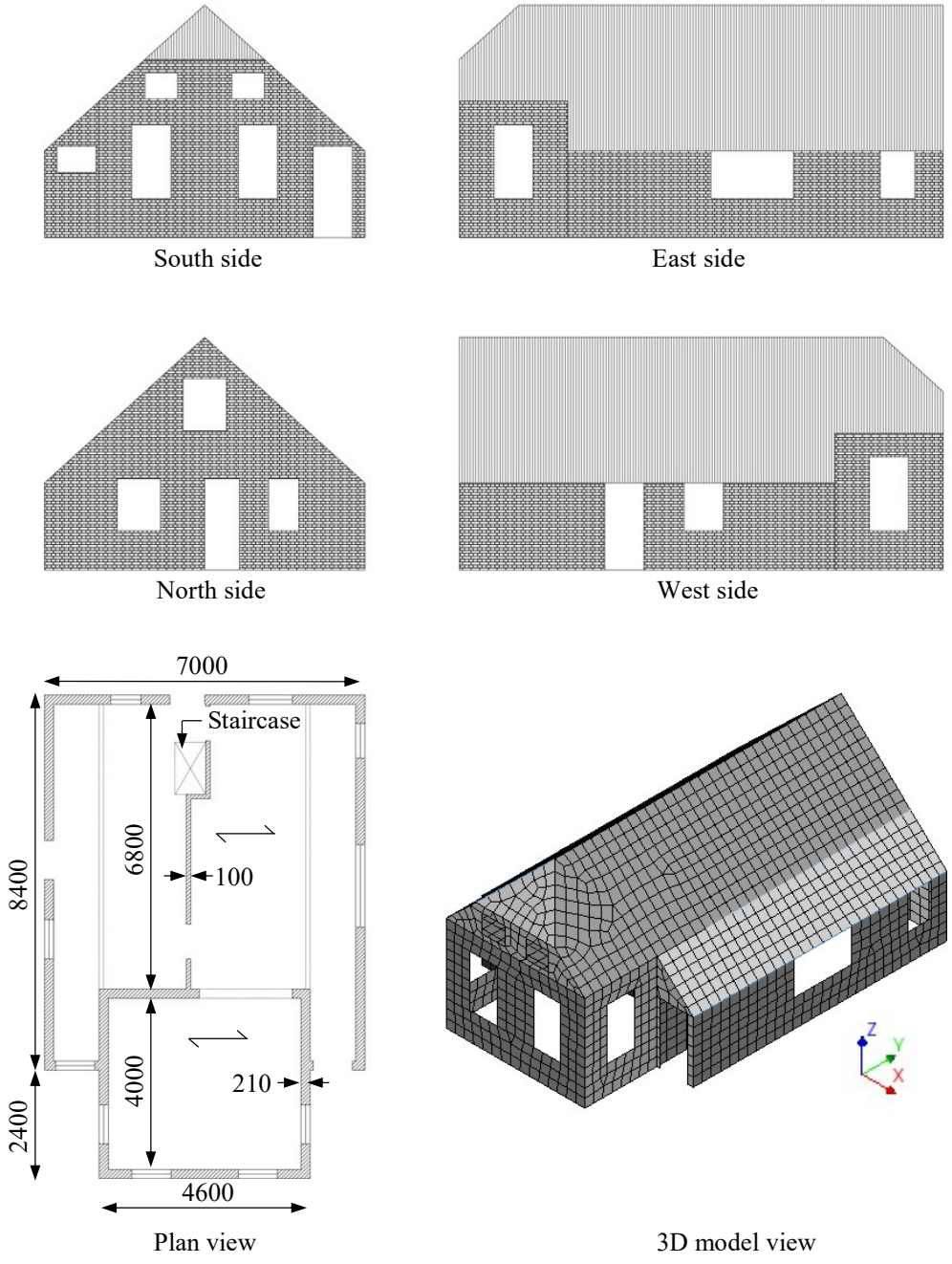

Figure 15: Main properties and geometry of the case-study building.

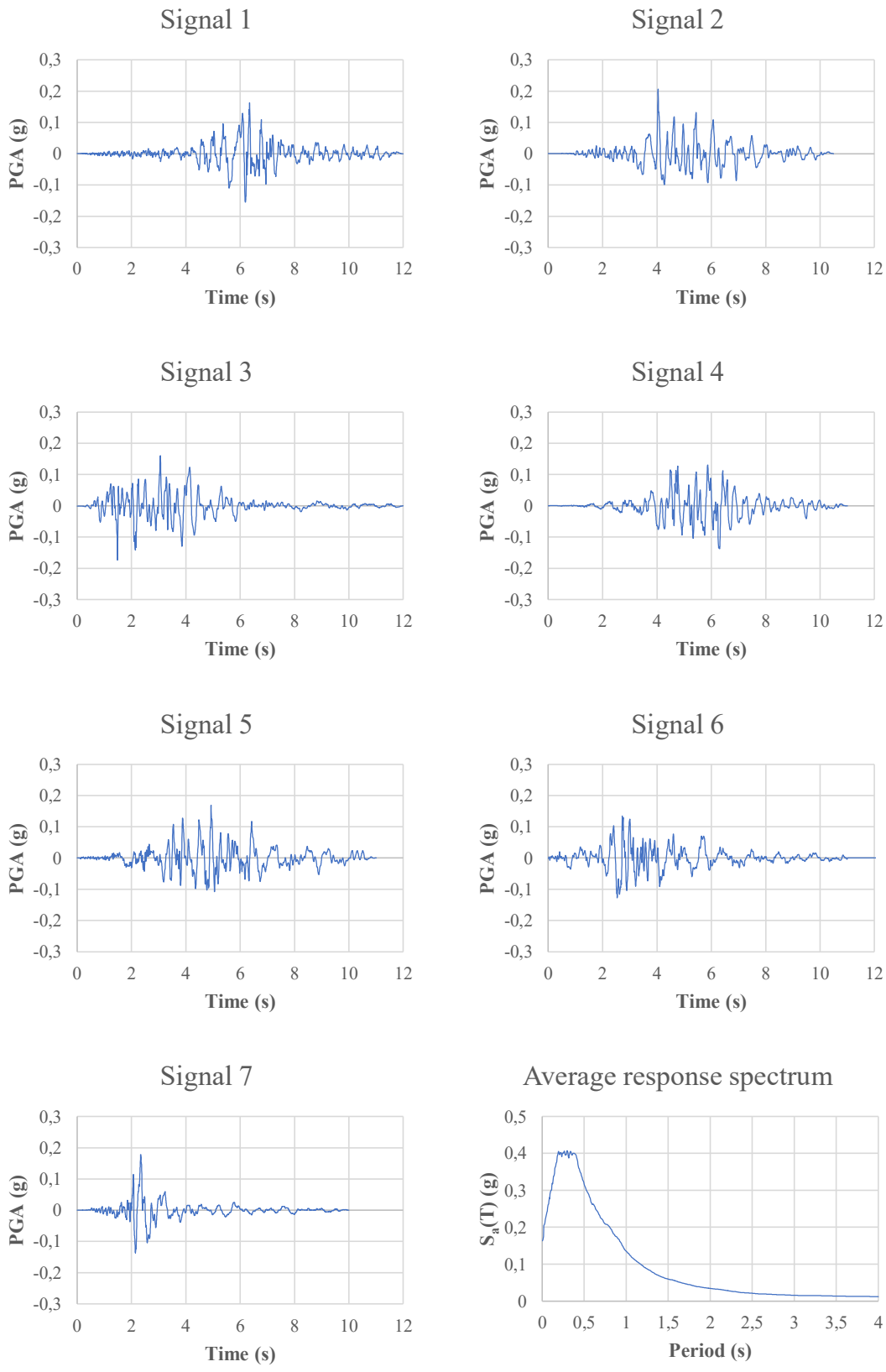

Figure 16: Adopted signals for time-history analyses; their average response spectrum is also reported. Data from NPR 9998 Webtool [35].

The following modelling strategies were adopted for the building with retrofitted floors:

- In the configuration with diaphragms retrofitted by casting a concrete slab on them, the floors were also modelled with linear elastic orthotropic shell elements, having the properties of structural reinforced concrete (Table 4). The thickness of the slab was 50 mm, as it would commonly be realized in practice [1], [6], [27]-[30].
- For the configuration featuring floors retrofitted with plywood panels, the modelling strategy discussed in section 4.2 was adopted: besides the linear elastic orthotropic shell elements, also the nonlinear macro-elements were present. The retrofitting interventions on the diaphragms were designed according to the global in-plane capacity of the piers, and conservative out-of-plane drift limits for the walls. The maximum base shear of the house (approximately 450 kN) was evaluated through a preliminary pushover analysis applied to the configuration with stiff diaphragms, and then the loads at floor and roof level were estimated through the lateral force method. The retrofitting intervention was designed accordingly, providing sufficient strength to activate in-plane failure mechanisms, but at the same time deflection capacity. With regard to this latter aspect, to prevent out-of-plane walls failure, the maximum midspan displacement, at which the diaphragms reached their strength, was fixed at 2% of the out-of-plane walls (or gables, for the roof) height. This value is in line with the 2.5% global drift suggested by New Zealand standards [37], which includes, however, also the displacement contribution of the in-plane walls. The potential stiffening effect of the out-of-plane walls was conservatively not taken into account, also because of the presence of large openings. Besides, use of dry screed made of loose material was assumed. Table 5 reports the properties of the retrofitted diaphragms adopted as input for the numerical model.

Table 2: Properties adopted for masonry shell elements based on [31]-[33].

Property	Value
Young modulus E_x parallel to bed joint(MPa)	1500
Young modulus E_y perpendicular to bed joint (MPa)	2000
Shear modulus G_{xy} (MPa)	800
Mass density ρ (kg/m^3)	2000
Bed joint tensile strength f_t (MPa)	0.15
Fracture energy in tension G_{F1} (N/mm)	0.01
Compressive strength f_c (MPa)	14
Fracture energy in compression G_c (N/mm)	30
Friction angle (°)	34
Cohesion (MPa)	0.2
Fracture energy in shear (N/mm)	0.1

Table 3: Properties adopted for the shell elements (thickness = 18 mm) representing the flexible diaphragms.

Property	Value		
	4.0×4.6 m floor	4.6×6.8 m floor	Roof
Young moduli E_x, E_y, E_z (MPa)	978000	620000	405000
In-plane shear modulus G_{xy} (MPa)	12	7	6
Shear moduli G_{xz}, G_{zy} (MPa)	61125	38750	25312
Mass density ρ (kg/m^3)	9440	9270	6170

Table 4: Properties adopted for the shell elements (thickness = 68 mm) representing the concrete slabs.

Property	Value		
	4.0×4.6 m floor	4.6×6.8 m floor	Roof
Young moduli E_x, E_y, E_z (MPa)	30000	30000	30000
Shear moduli G_{xy}, G_{xz}, G_{zy} (MPa)	12500	12500	12500
Mass density ρ (kg/m^3)	4336	4290	4250

Table 5: Properties adopted for the macro-elements and shell elements (thickness = 36 mm) representing the diaphragms retrofitted with plywood panels.

Property	Value		
	4.0×4.6 m floor	4.6×6.8 m floor	Roof
Macro-elements			
ε_{max}	0.027	0.019	0.012
σ_{max} (MPa)	12700	21200	13700
K_0 (MPa)	2490000	5980000	5980000
Shell elements			
Young moduli E_x, E_y, E_z (MPa)	122000	77500	50700
In-plane shear modulus G_{xy} (MPa)	0.1	0.1	0.1
Shear moduli G_{xz}, G_{zy} (MPa)	7640	4840	3170
Mass density ρ (kg/m^3)	4940	4860	3310

5.3 Results of the time-history analyses and discussion

The three configurations of the house were subjected to the seven signals shown in Fig. 16, by progressively scaling them until collapse. The results in terms of PGA at collapse of the configurations are presented in Fig. 17. The reference design response spectrum (2475 years return period) for the location of the house (Godlinze) corresponded to an expected maximum PGA of 0.17g: as can be noticed, the as-built configuration already collapsed at this level of intensity under almost all signals, making a retrofitting intervention necessary to increase the seismic performance of the house. Instead, the floors stiffened with a concrete slab greatly improve the capacity of the building, but the best performance is obtained with the plywood panels overlay, in both directions. The latter retrofitting intervention is easily applicable, light, reversible, and provides a beneficial energy dissipation to the diaphragms, improving even more the seismic capacity of the house.

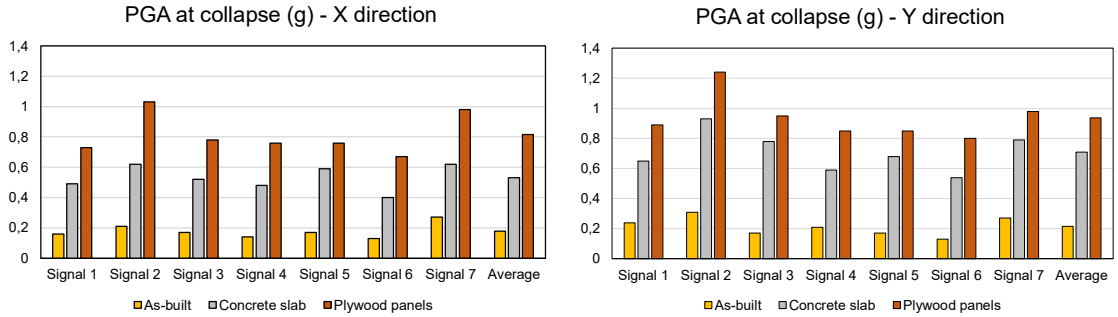

Figure 17: PGA at collapse for the three configurations in the *x* (left) and *y* direction (right).

The effect of the diaphragms on the response of the building is represented in Fig. 18: the base shear-displacement curves are reported at collapse, and refer, as a representative example, to signal 1 applied in the *x* direction (the weakest); the control node for displacement corresponds to the centre of mass of the roof. The as-built configuration shows a very flexible response: the floors undergo large displacements at an already limited signal amplitude, and the in-plane walls are not brought into play. Besides, the crack pattern (Fig. 18a) shows a partial out-of-plane collapse of the 100 mm thick central wall, and of the north gable, probably due to torsional effects.

A very different situation is noticeable with the floors retrofitted with concrete slabs. In this case, the failure of the building is fully related to the in-plane walls, and a beneficial redistribution of horizontal loads is achieved among the various walls; the force-displacement graph also confirms a typical in-plane failure of masonry (Fig. 18b).

A hybrid response between the first two configurations is obtained when the floors are retrofitted with plywood panels: a larger displacement capacity of the diaphragms together with an in-plane failure of the walls is noticeable (Fig. 18c). The crack pattern is similar to that observed for the concrete slab configuration, with a slightly higher amount of damage in the out-of-plane walls, because of the lower stiffness of the floors. Yet, the beneficial dissipative effect of the diaphragms leads to a 30% higher performance of the building in terms of PGA.

The possibility of withstanding more intense earthquakes does not only depend on the lower seismic mass provided by the reversible retrofitting intervention, but also because of its energy dissipation capacity. In fact, first of all, the higher mass of the concrete slab has a beneficial effect on the in-plane capacity of the wall, which is increased due to the larger vertical precompression applied. Secondly, by performing a modal analysis, the fundamental period of the house retrofitted with concrete slabs resulted as 0.1 s, while for the configuration with diaphragms strengthened with plywood panels it was 0.14 s. In both cases, the structure in the elastic phase is stiff, as expected when studying a low-rise masonry building; however, the plateau of the design average response spectrum starts at a period of 0.19 s (Fig. 16). Since the displacement capacity of the diaphragms retrofitted with plywood panels immediately brings into play their nonlinearity (including pinching cycles and energy dissipation), this configuration has a rapid increase of its period, and becomes quickly subjected to the maximum spectral acceleration. When concrete slabs are present, the diaphragms can be regarded as infinitely stiff, thus the response is approximately linear elastic until the in-plane capacity of the weakest wall is reached. The combination of a higher precompression on the walls (and therefore a higher in-plane strength) with a limited displacement capacity, compared to the floors retrofitted with plywood panels, implies a slower evolution of the period due to nonlinearities, and the spectral plateau is reached at a later stage. Nevertheless, the reversible retrofitting still shows a higher capacity, confirming its beneficial dissipative role.

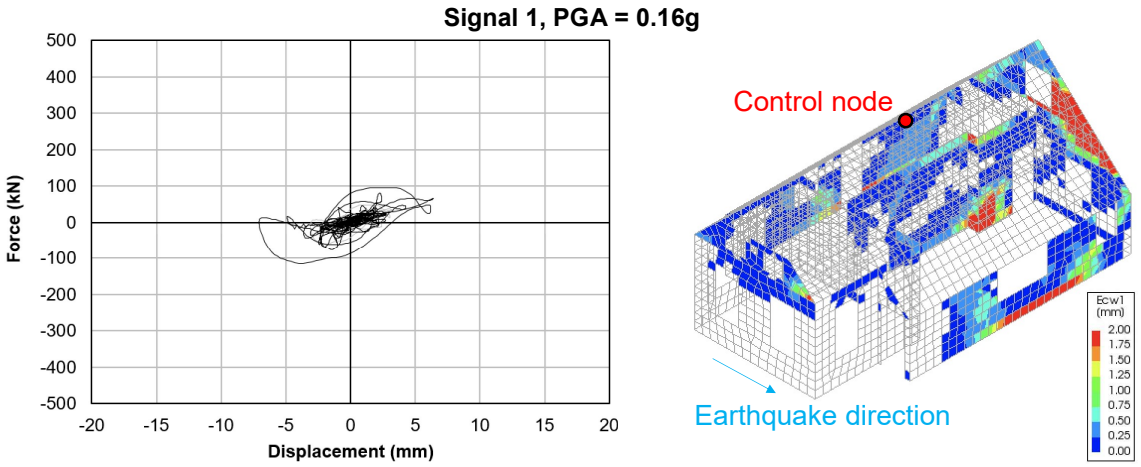

(a)

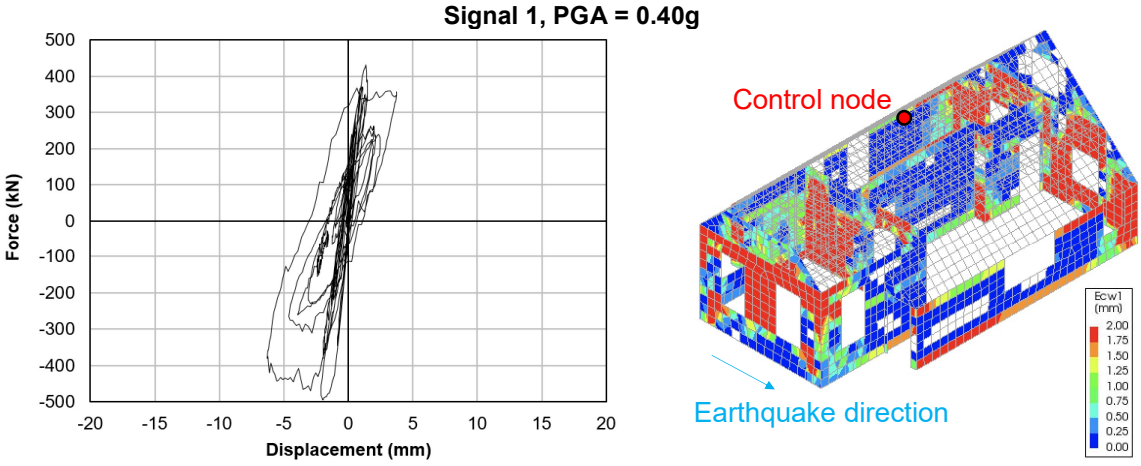

(b)

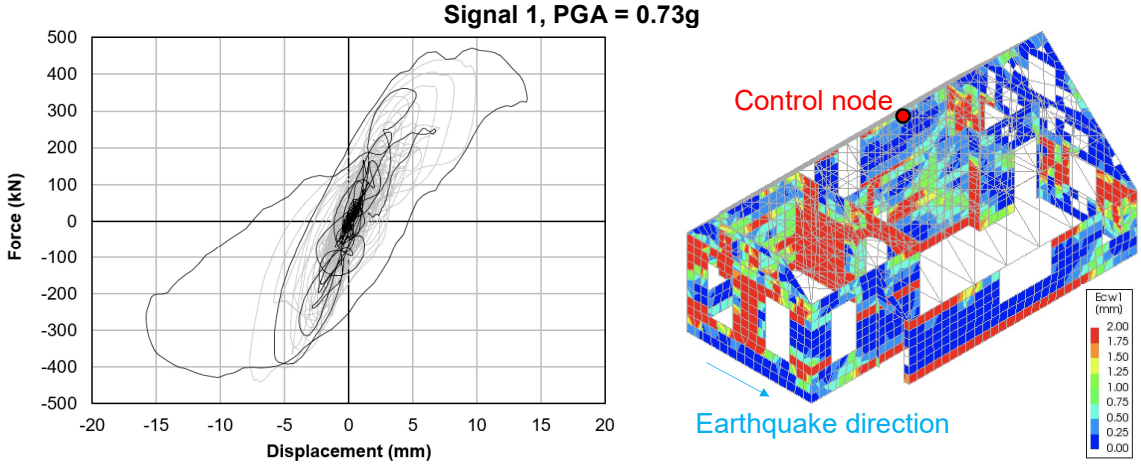

(c)

Figure 18: Base shear vs. roof displacement response and crack opening (Ecw1) pattern of the three configurations: as-built (a), floors strengthened with concrete slabs (b), diaphragms retrofitted with plywood panels (c).

The dissipation provided by the floors is furtherly highlighted by Figs. 19 and 20, both showing the positive effect of the plywood panels retrofitting on the response of the building. Fig. 19 compares the in-plane behaviour of the most solicited wall at the collapse PGA for the concrete slab configuration, and the same response with the plywood panels overlay. As can be noticed, in the latter case the wall has not yet reached its capacity, but has just started to behave nonlinearly. Fig. 20 shows the total hysteretic energy dissipated by the structural components of the house: the amount of energy dissipated by the floors is relevant and, especially in the early phase of an earthquake, this can helpfully reduce in-plane loads on the walls.

As last consideration, in [25] a value of equivalent hysteretic damping ratio $\xi = 15\%$ was determined for the diaphragms retrofitted with plywood panels. The difference in PGA at collapse between the configuration with stiff floors and that with the dissipative diaphragms was on average 30% (Fig. 17). This result appears to confirm the obtained 15% damping ratio: if the floors were retrofitted with plywood panels, and for a simplified modelling (e.g. a pushover analysis) they were assumed as stiff, their dissipative contribution could be taken into account by considering an overdamped spectrum reduced by the factor $\eta = [10/(5+\xi)]^{1/2}$ [38]. It is interesting to notice that $\eta = 0.71$ for $\xi = 15\%$, a value suggesting that the collapse response spectrum could indeed correspond to approximately 30% higher spectral acceleration when a dissipative retrofitting of the floors is designed, and in addition to the further nonlinear contribution of the in-plane masonry walls.

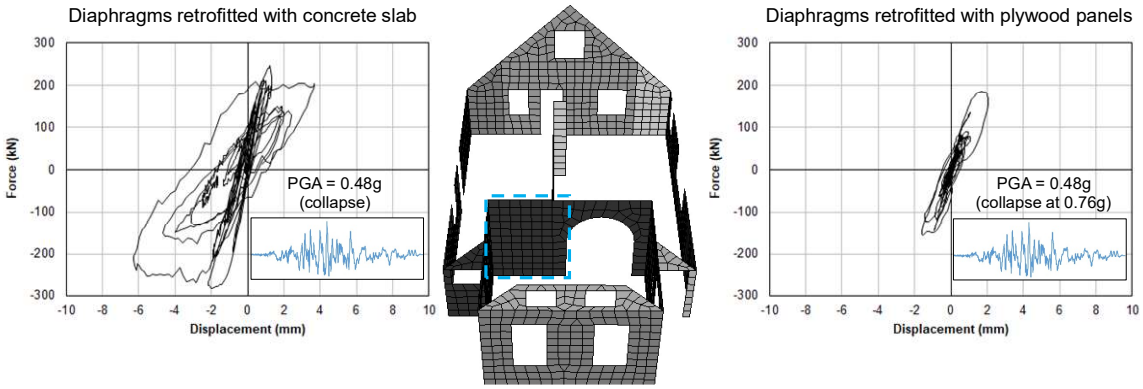

Figure 19: Comparison between the in-plane response of the most solicited wall under the application of signal 4 in the configuration having floors strengthened with concrete slabs (left) and with plywood panels (right).

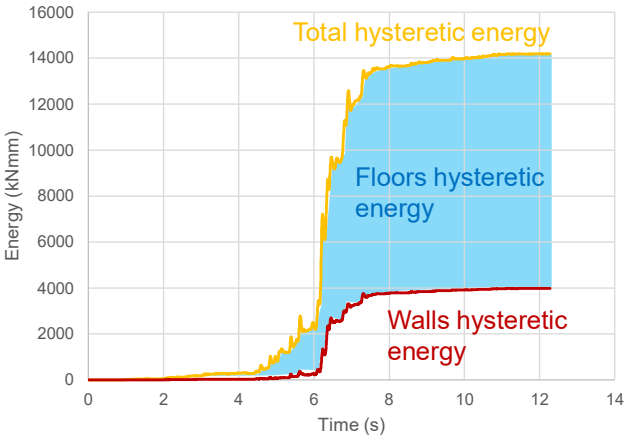

Figure 20: Hysteretic energy vs. time response under seismic signal 1 for the building having floors retrofitted with plywood panels: the dissipative role of the diaphragms is evident.

6 SUMMARY AND CONCLUSIONS

In this work, starting from an experimental campaign on as-built and strengthened timber diaphragms, the analytical and numerical modelling of the retrofitted floors was presented, including an application to a case-study existing building.

The strengthening technique, consisting of an overlay of plywood panels screwed along their perimeter to the existing sheathing, showed a great improvement in strength, stiffness and energy dissipation of the diaphragms. In order to enable the design of the proposed retrofitting method, and to account for the nonlinear and dissipative response of the floors, an analytical model was formulated, starting from the load-slip behaviour of the single screws fastening plywood panels and planks. The analytical model shows good agreement with the experimental results, and can be adopted to determine the relevant seismic properties of the retrofitted diaphragms.

The formulated model opened up the opportunity to implement a user-supplied subroutine in the software DIANA FEA: the subroutine validation demonstrated that an accurate numerical modelling of the in-plane response of the floors can be achieved. Then, the proposed retrofitting intervention was applied to the case-study of an existing building, and the seismic response was compared to both that of the as-built house, and that of a configuration in which the floors were stiffened with concrete slabs. The numerical time-history analyses showed that the diaphragms retrofitted with plywood panels can greatly improve the seismic capacity of the building, mainly because high energy dissipation is provided, and already at limited deflections. This allows to beneficially dampen the in-plane loads on the walls, obtaining the best performance, even in comparison to the configuration retrofitted with concrete slabs.

Therefore, the choice of light, reversible and dissipative retrofitting like the proposed one could be not only a more suitable technique for seismic strengthening of buildings belonging to architectural heritage, but also more beneficial in improving seismic capacity compared to stiffer, not reversible, and less sustainable techniques.

REFERENCES

[1] M. Piazza, C. Baldessari, R. Tomasi, The Role of In-Plane Floor Stiffness in the Seismic Behaviour of Traditional Buildings. *14th World Conference on Earthquake Engineering*, Beijing, 2008.

[2] C. Modena, M.R. Valluzzi, E. Garbin, F. da Porto, A strengthening technique for timber floors using traditional materials. *Proceedings of the Fourth International Conference on Structural Analysis of Historical Constructions SAHC 04*, Padua, Italy, 10–13 November 2004, pp. 911–921, 2004.

[3] M.R. Valluzzi, E. Garbin, M. Dalla Benetta, C. Modena, In-Plane Strengthening of Timber Floors For The Seismic Improvement Of Masonry Buildings. *11th World Conference on Timber Engineering*, Riva del Garda, 2010.

[4] M.R. Valluzzi, E. Garbin, M. Dalla Benetta, C. Modena, Experimental Assessment and Modelling of In-Plane Behaviour of Timber Floors. D. D'Ayala and E. Fodde (Eds.), *Proceedings of the VI International Conference on Structural Analysis of Historic Construction, SAHC 08*, 2–4 July 2008, Bath, UK, 2008, pp. 755-762.

[5] N. Gattesco, L. Macorini, High reversibility technique for in-plane stiffening of wooden floors. D. D'Ayala and E. Fodde (Eds.), *Proceedings of the VI International Conference*

on Structural Analysis of Historic Construction, SAHC 08, 2–4 July 2008, Bath, UK, 2008, pp. 1035–1042.

[6] M. Corradi, E. Speranzini, A. Borri, A. Vignoli, In-Plane Shear Reinforcement of Wood Beam Floors With FRP. *Composites: Part B* **37**, 310-319, 2006.

[7] J.M. Branco, M. Kekeliak, P.B. Lourenço, In-Plane Stiffness of Timber Floors Strengthened with CLT. *European Journal of Wood Products* **73**, 313-323, 2015.

[8] A. Gubana, M. Melotto, Experimental tests on wood-based in-plane strengthening solutions for the seismic retrofit of traditional timber floors, *Construction and Building Materials* **191**, 290–299, 2018.

[9] E. Rizzi, M. Capovilla, M. Piazza, I. Giongo, In-plane behaviour of timber diaphragms retrofitted with CLT panels. Chapter in book: R. Aguilar et al. (Eds.): *Structural Analysis of Historical Constructions*, RILEM Bookseries 18, pp. 1613-16222, 019

[10] D.F. Peralta, M.J. Bracci, M.B.D. Hueste, Seismic Behavior of Wood Diaphragms in Pre-1950s Unreinforced Masonry Buildings. *Journal of Structural Engineering* **130**, 2040-2050, 2004.

[11] A. Brignola, S. Pampanin, S. Podestà, Experimental Evaluation of the In-Plane Stiffness of Timber Diaphragms. *Earthquake Spectra*, Volume 28, No. **4**, 1–23, 2012.

[12] A. Wilson, P.J.H. Quenneville, J.M. Ingham, In-Plane Orthotropic Behavior of Timber Floor Diaphragms in Unreinforced Masonry Buildings. *Journal of Structural Engineering* **140**, 2014.

[13] E. Rizzi, I. Giongo, J. Ingham, D. Dizhur D., Testing and Modeling In-Plane Behavior of Retrofitted Timber Diaphragms. *Journal of Structural Engineering*, vol. 146, **2** , 2020.

[14] M. Mirra, G. Ravenshorst, J.W. van de Kuilen, Experimental and analytical evaluation of the in-plane behaviour of as-built and strengthened traditional wooden floors. *Engineering Structures* **211**, 2020.

[15] A. Gubana, State-of-the-Art Report on high reversible timber to timber strengthening interventions on wooden floors. *Construction and Building Materials* **97**, 25-33, 2015.

[16] M. Mirra, G. Ravenshorst, P. de Vries, J.W. van de Kuilen, An analytical model describing the in-plane behaviour of timber diaphragms strengthened with plywood panels. *Engineering Structures* **235**, 2021.

[17] D. Ferreira, ed., DIANA – Finite element analysis. User's manual release 10.4. DIANA FEA BV, Delft, The Netherlands, 2020.

[18] ISO 16670:2003. Timber structures — Joints made with mechanical fasteners — Quasi-static reversed-cyclic test method. ISO (International Organization for Standardization)

[19] R.O. Foschi, Load-Slip Characteristics of Nails. *Wood Science* **17**, 69-77, 1974.

[20] EN 12512:2001. Timber Structures – Test Methods – Cyclic Testing of Joints Made with Mechanical Fasteners. CEN (European Committee for Standardization).

[21] P. Dubas, E. Gehri, T. Steurer, Einführung in die Norm SIA 164 (1981) – Holzbau. Publication No. 81-1, Baustatik und Stahlbau, ETH Zürich, Switzerland, 1981.

[22] EN 1995-1-1:2004+A2:2014. Eurocode 5: Design of timber structures - Part 1-1: General - Common rules and rules for buildings. CEN (European Committee for Standardization).

[23] K.W. Johansen, Theory of timber connections. Publ. 9 Bern. International Association of Bridge and Structural Engineering, 1949.

[24] EN 409:2009. Timber structures - Test methods - Determination of the yield moment of dowel type fasteners. CEN (European Committee for Standardization).

[25] M. Mirra, G. Ravenshorst, J.W. van de Kuilen, Dissipative properties of timber diaphragms strengthened with plywood panels. *Proceedings of the 16th World Conference on Timber Engineering*, Santiago, Chile, 9-12 August 2021. (submitted)

[26] S. Lagomarsino, A. Penna, A. Galasco, S. Cattari, TREMURI program: An equivalent frame model for the nonlinear seismic analysis of masonry buildings. Engineering Structures 56, 1787-1799, 2013.

[27] I. Giongo, M. Piazza, R. Tomasi, Pushover analysis of traditional masonry buildings: influence of refurbished timber-floors stiffness. *SHATIS'11 International Conference on Structural Health Assessment of Timber Structures* - Lisbon, Portugal, June 2011.

[28] R. Scotta, D. Trutalli, L. Marchi, L. Pozza, M. Mirra, Seismic response of masonry buildings with alternative techniques for in-plane strengthening of timber floors. *Revista Portuguesa de Engenharia de Estruturas*. Ed. LNEC. Série III, no **4**, 2017

[29] R. Scotta, D. Trutalli, L. Marchi, L. Pozza, M. Mirra, Non-linear time history analyses of unreinforced masonry buildings with in-plane stiffened timber floors. *Proceedings of the 17th ANIDIS Conference*, Pistoia, Italy, 2017.

[30] D. Trutalli, L. Marchi, R. Scotta, L. Pozza, Dynamic simulation of an irregular masonry building with different rehabilitation methods applied to timber floors. M. Papadrakakis, M. Fragiadakis (eds.), *Proceedings of the 6th ECCOMAS Thematic Conference on Computational Methods in Structural Dynamics and Earthquake Engineering*, Rhodes Island, Greece, 15-17 June 2017.

[31] F. Messali, G. Ravenshorst, R. Esposito, J.G. Rots, Large-scale testing program for the seismic characterization of Dutch masonry walls. *Proceedings of 16th World Conference on Earthquake (WCEE)*, Santiago, Chile, 9-13 January 2017.

[32] S. Jafari, J.G. Rots, R. Esposito, F. Messali, *Characterizing the Material Properties of Dutch Unreinforced Masonry*. Procedia Engineering **193**, p. 250-257, 2017.

[33] F. Messali, M. Longo, Influence of dormers on the seismic performance of a detached house: case study Kwelder 1, Loppersum. Report number B2B-R04, Version 01, Delft University of Technology, 21 January 2021.

[34] G.M.A. Schreppers, A. Garofano, F. Messali, J.G. Rots. DIANA validation report for masonry modelling. DIANA FEA BV and Delft University of Technology, 2017

[35] Webtool NPR 9998 (https://seismischekrachten.nen.nl). Nederlands Normalisatie-instituut (NEN), 2021.

[36] NEN-EN 1990:2002+A1:2019+NB:2019. Grondslagen van het constructief ontwerp (Dutch national version of Eurocode 0). Nederlands Normalisatie-instituut (NEN).

[37] NZS 1170.5. Structural design actions, Part 5: Earthquake actions – New Zealand, Standards New Zealand, Wellington, 2004.

[38] EN 1998-1:2004. Eurocode 8: Design of structures for earthquake resistance – Part 1: General rules, seismic actions and rules for buildings. CEN (European Committee for Standardization).